WELDING RESEARCH

SUPPLEMENT TO THE *WELDING JOURNAL*, MARCH 2004
Sponsored by the American Welding Society and the Welding Research Council

Activated Diffusion Brazing Technology for Manufacture of Titanium Honeycomb Structures — A Statistical Study

A linear regression method was used to establish the relationship between process parameters and the properties of the brazed joint

BY X. HUANG AND N. L. RICHARDS

ABSTRACT. Titanium honeycomb structures were manufactured using activated diffusion brazing (ADB) technology. Titanium Alloy Ti-6Al-4V was used as face sheets to join with honeycomb core in three core sizes (¼, ½ and ¾ in.). A design of experiments was used to determine the experimental matrix, and 48 tests were conducted under various process conditions. A proprietary filler metal foil was used with the process and all the welded structures were subjected to nondestructive evaluation, tensile test, and metallographic evaluation. The relationships between the process variables (temperature, time, load pressure, face sheet thickness, core size, and number of filler metals) and the properties of the brazed honeycomb panels were established using the linear regression method. An important feature of the ADB panels was that most of the failures occurred in the honeycomb core, suggesting that the braze interface was no longer the weakest link as compared to other joining methods such as vacuum brazing of aluminum alloys.

Introduction

Honeycomb sandwich structures have been used successfully since the early 1950s in aircraft, space, and naval applications due to their remarkable compressive strength-to-weight ratio, high temperature capability, and excellent corrosion resistance. A typical three-layer structure of a honeycomb panel consists of two face sheets and a honeycomb core situated between them. The honeycomb is usually produced from foil with cell walls joined together using resistance welding. In honeycomb structures, the face sheets are the prime load-bearing element. The goal in panel design and manufacture is to achieve complete stabilization of the component faces since the desired compressive strength can then be attained with thinner gauge materials. The honeycomb core provides buckling resistance for the structure while at the same time transmitting shear forces. Additionally, inherent to honeycomb structures are remarkable stiffness, vibration damping, thermal, acoustic, and insulation properties. The application of honeycomb structures for use at elevated temperatures is limited only by the properties of the base materials and type of joining method used to manufacture them.

There are two common types of lightweight metallic honeycomb structures that have been used in the aerospace industry. The first type is an aluminum (Al) structure manufactured using adhesive bonding or brazing technologies (Ref. 1). Application of these Al structures is limited to moderate temperature use (typically <200°C) due to the polymeric bonding materials used or the low melting point filler metal employed. The second type is a titanium (Ti) honeycomb structure joined to face sheets using vacuum brazing technology. Brazing of the Ti structure can be achieved using several classes of braze alloy: 1) aluminum alloys (Refs. 2, 3), 2) Ag-based alloys (Ref. 4), 3) Ti-Cu (Refs. 5, 6) or Ti-Cu-Ni/Zr alloy (Refs. 7–10), and 4) use of Cu-Ni, or Cu-Ni-Ti joining systems (Refs. 11–13). The disadvantages of using silver- and aluminum-based brazing alloys include the formation of brittle intermetallics during the brazing cycle and while in service, poor uniformity of the braze joint due to the free-running nature of the braze alloy at brazing temperature, galvanic corrosion, and a lower application temperature (<300°C) when compared to Ti-Cu-Ni/Zr brazed structures (Ref. 9). Joints that have to sustain higher temperatures in service are therefore primarily brazed with Ti-Cu-Ni/Zr. In 1959 Lynch et al. (Ref. 5) discussed a Ti-Ti bond in an unknown alloy of Ti using a 0.025-mm-thick Ni interlayer. Further Ti-Cu research in 1971 resulted in the NOR-TI-BOND process (Ref. 6) using an electrolytically deposited Cu interlayer. The process was used for joining titanium I and T beams.

In brazing of Ti structures using a Ti-Cu-Ni alloy system, brazing alloys of various compositions and forms (foil, coating, powder, and paste) are used with the purpose of lowering the brazing temperature, decreasing the brazing time, reducing/eliminating undesirable phases formed at the joint, and achieving high mechanical properties of the joint. There have been a number of studies carried out using Ti-15Cu-15Ni brazing foil, all exhibiting good wetability and a high resultant joint strength. However, this alloy has also been reported to form remark-

KEY WORDS

Aerospace
Aluminum
Brazing
Diffusion Brazing
Honeycomb Structures
Titanium

X. HUANG is with Department of Mechanical and Aerospace Engineering, Carleton University, Ottawa, Ontario, Canada. N. L. RICHARDS is with Department of Mechanical and Industrial Engineering, University of Manitoba, Winnipeg, Manitoba, Canada.

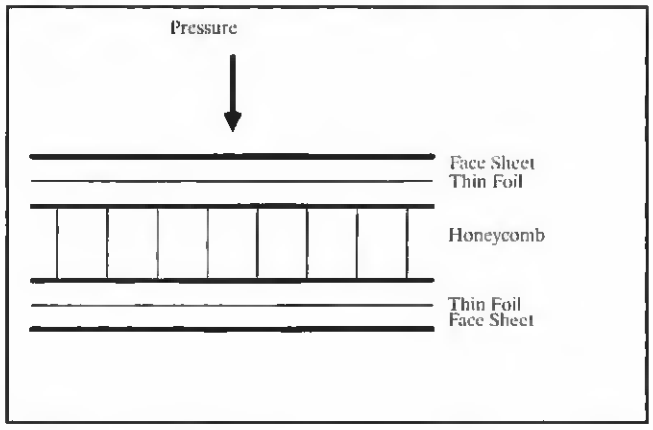

Fig. 1 — Layout of honeycomb panels.

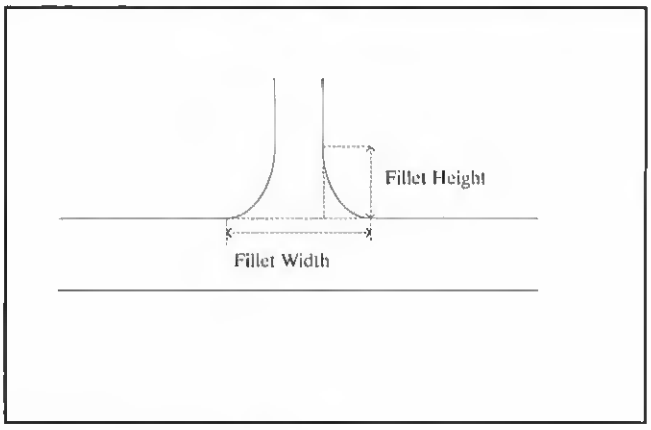

Fig. 2 — Measurement of fillet size.

able porosity as the alloy melts in three separate stages (Refs. 7–10). The liquid interface bonding (LID) techniques developed initially by Rohr and similarly by Rolls-Royce were described in Refs. 11–13 with various Ti-Cu-Ni joints for aerospace applications such as hollow fan blades. Limited technical data are available in publications; however, Fitzpatrick emphasized the qualitative factors influencing joining such as temperature, pressure, time, surface roughness, and interlayer type. More recently, an amorphous Ti-Zr-based filler metal was produced in ribbon form in a wide variety of compositions using rapid solidification technology (Ref. 8). While the melting point has been reduced considerably to 800–820°C for Ti-Zr-Cu/Ni-based filler metals, in comparison with Ti-Cu-Ni alloy system (916°C for Ti-21Ni-14Cu), the corrosion resistance of Ti-42.5Zr-10Cu-5Ni and Ti-35Zr-15Cu-15Ni alloys was considered inferior as compared to Ti-15Cu-15Ni alloy (Ref. 15). While most of the research work conducted in welding Ti alloys has used a single layer of alloy as filler, some have studied diffusion welding of Ti alloy to Fe-Ni based alloys using two layers of pure metals. For example, layers of 25-μm Ta and 25-μm Ni were used to join IMI 829 to IN 907 at 975°C/1 h with the joint strength achieving 75% of the base materials (Ref. 16).

Brazing of titanium alloys for high-temperature application can be carried out using a vacuum furnace or induction heating within a vacuum system (Ref. 4). The advantage of induction heating is that the entire assembly does not need to be heated and turnaround time is quicker. However, it is only suitable for some particular configurations of components, such as ducts and fittings. In the majority of the cases where complicated components are to be joined, a vacuum furnace has always been the choice.

The microstructure in the joint depends primarily on the filler material used and the process parameters. During brazing of Ti-6Al-4V using Ti-21Ni-14Cu at 960°C, diffusion of Cu and Ni from the filler metal into the equiaxed α plus intergranular β structure of substrate causes the lamellar Widmanstätten structure to form. The intermetallic Ti_2Ni phase, which exists in the filler metal, diminishes as diffusion progresses, while Ti_2Cu phase was found in the brazing layer (Ref. 7). Diffusion brazing of Ti-6Al-4V with Ti-Cu-Zr at 900°C (1173 K)/1 h produced a brazing layer with an acicular $Ti(Zr)_2Cu$ and α-Ti with dissolved Zr (Refs. 9–10). The cooling rate has also been observed to affect the microstructure in the interface layer. Slow cooling rates have been observed to result in brittle hexagonal Cu_2TiZr phases when 15Ti-25Zr-50Cu was used to braze Ti-6Al-4V at 900°C (Ref. 9).

The joining of Ti alloys for high-temperature application can also be achieved using solid-state diffusion brazing. However, with solid-state, the Ti plate is often deformed in the vicinity of the brazing layer owing to the high temperature and pressure (Ref. 10). Additionally, solid-state diffusion brazing has not been used in joining honeycomb structures as the honeycomb nodes cannot be filled during the solid-state process.

The limitations associated with brazing and the solid-state diffusion brazing process can be eliminated using activated diffusion brazing (ADB). In activated diffusion brazing, a thin foil of a selected alloy (a variation of Ti-Ni-Cu) is placed between the honeycomb and face sheets as illustrated in Fig. 1. When heat is applied to the structure, this alloy reacts with the base metals to form a liquid eutectic intermediate layer between the honeycomb core and face sheet. However, this layer rapidly dissolves into the base metal by diffusion leaving the honeycomb joined to the face sheet. Because of the thin layer of foil used, the joint zone created is very narrow and contains transition phases, which can be eliminated with further heat treatment. As such, the important features of ADB technology are the elimination of the original mating surface, the use of moderate pressure without deforming, the core material, and the relatively low brazing temperature used.

The majority of the research on ADB of Ti has been concerned with microstructural aspects rather than the key process characteristics of the process. As discussed above, Fitzpatrick (Refs. 12, 13) mentioned qualitative factors, but gave no indication of quantitative factors controlling the process. The present investigation was undertaken to remedy this fact, with process parameters varied in a statistically designed series of experiments and the key design mechanical properties of the joints evaluated. For each mechanical property, the key statistically significant process characteristics were evaluated and reported in the paper. To ensure process robustness, quantitative aspects controlling the key process characteristics are necessary for manufacturing control, especially in the quality-intensive manufacturing environment that pervades the aerospace industry.

Experimental

Initial Development

This study was carried out in two stages. In the first stage, preliminary experiments were carried out to find the range of working process parameters, including temperature, time, pressure, surface treatment, and amount of filler metal required to achieve adequate honeycomb node flow, elimination of intermetallics, and minimized face sheet distortion. Once established, an experimental matrix was designed using statistical methods to evaluate the relationship between process parameters and their effects on honeycomb structure properties.

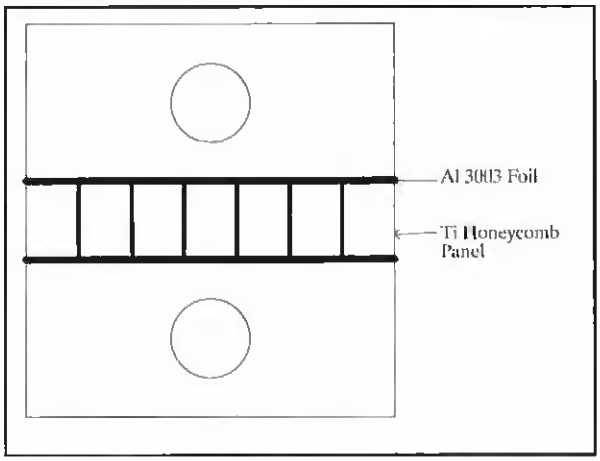

Fig. 3 — Flatwise tensile test fixture.

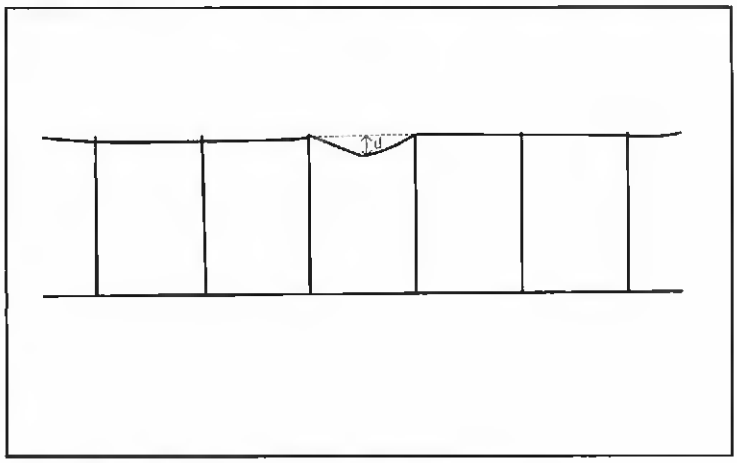

Fig. 4 — Measurement of honeycomb panel distortion d.

Prior to the statistical process development of ADB technology, initial examination was carried out to establish a baseline working process. The early trials used a 0.46-mm- (0.018-in.-) thick Ti-6Al-4V face sheet, corrugated honeycomb core of 9.5-mm (⅜-in.) cell size, 10-mm (0.4-in.) high and ADB foil. The face sheets were chemically cleaned and covered with layer of ADB foil. The honeycomb core was also chemically cleaned and then sandwiched between the two prepared face sheets to make up the assembly as shown in Fig. 1. Diffusion brazing trials were carried out in vacuum furnace (with atmosphere pressure $<4 \times 10^{-4}$ torr) at various temperature/time and pressure applied to the panel. All the panels were subject to visual, X-ray radiographic, and metallographic examinations. Based on this preliminary investigation, a design of experiment (DOE) was carried out as described previously to fully examine the ADB process.

Design of Experiment Using Statistical Method

For a quantitative evaluation of the effect of various variables on the properties of brazed joints, the number of experiments required was determined using design of experiment.

Based on the experimental design detailed in Appendix 1, nine furnace runs (denoted as ADB-1 to ADB-9) were conducted as detailed in Appendix 2 (2-1 to 2-9), with each run having the same temperature and cycle time. All brazing cycles were conducted in a vacuum furnace at a pressure lower than 10^{-4} torr.

Evaluation Method

X-Ray Radiography

All diffusion brazed honeycomb panels were evaluated using X-ray radiography in two dimensions, normal to the face sheet and at an angle to the surface, to determine defects such as number of nodes lacking filler metal.

Metallographic Examination

The brazed panels were machined into four 2 × 2 in. sections using the electron-discharge machining (EDM) method to minimize distortion to the honeycomb core. Once four sections were produced, one section was further electron-discharge machined perpendicularly to the honeycomb wall to produce samples for metallographic examination of diffusion layer thickness and filler size. A cold mounting method was utilized, again to prevent distortion to the structure. The specimens were prepared following standard polishing methods. Kroll's etchant was used to etch the specimens. Fillet size and diffusion layer thickness (as illustrated in Figs. 2 and 5c) were measured using an optical microscope and all the measurements were normalized using the known core and face sheet thicknesses.

Strength Test

Flatwise tensile strength was tested using the configuration shown in Fig. 3. The conventional method of bonding the honeycomb panel to the tooling fixture using adhesive was not successful as failure always occurred at the adhesive joint. In order to test the true strength of ADB panels, a 3003 Al foil was used to braze the panel to the tooling (made from Ti-6Al-4V bar material) and it was proven to be very successful.

Distortion Measurement

The distance (d) between the localized low point and the adjacent area was measured as shown in the schematic diagram of Fig. 4. The largest value of distortion measured on each panel was used to represent the distortion for panels processed at various conditions.

Results

The quantitative results obtained from this study are summarized in Table 1. Linear regression method as described in the following section was used to analyze the results.

Linear Regression Method

A statistical analysis software (StatSoft) was used to analyze the correlation between the independent variables and the dependent variables in a multiple linear regression manner. The linear regression gives the general relationship between several independent variables and a dependent variable. A line in a two-dimensional or two-variable space is defined by the equation $Y=a+hX$, where the constants a and h are the intercept and slope of the regression. In the multivariant case, when there is more than one independent variable, the regression line cannot be visualized in two-dimensional spaces, but can be computed. In general, multiple regression procedures will estimate a linear equation of the form:

$$Y = a + b_1x_1 + b_2x_2 + b_3x_3 + b_4x_4 + \ldots\ldots\ldots + b_nx_n$$

Statistical Significance — p Level

The statistical significance of results is an estimated measure of the degree to which it is true. The value of the p level represents a decreasing index of the reliability of the result. The higher the p level, the less we can believe that the observed relationship between the variables in the

Table 1 — Summary of Test Results

	Distortion (mm)	Fillet Width (mm)	Diffusion Layer (mm)	No. of Nodes Lacking Flow	Tensile Strength (MPa)
ADB1-1	0.1778	0.3556	0.0991	2	14.44
ADB1-2	0.0000	0.5842	0.0762	19	13.79
ADB1-3	0.0508	0.5842	0.0508	3	15.08
ADB1-4	0.0013	0.3302	0.0711	6	13.79
ADB2-1	0.0076	0.2032	0.1041	14	15.59
ADB2-2	0.0381	0.3048	0.0864	0	15.51
ADB2-3	0.0229	0.635	0.0991	4	18.39
ADB2-4	0.0229	0.381	0.1016	10	17.41
ADB3-1	0.0254	0.6096	0.1016	0	15.02
ADB3-2	0.0254	0.4572	0.1067	2	14.22
ADB3-3	0.0254	0.5842	0.1143	0	14.22
ADB3-4	0.0508	0.4064	0.1016	0	14.36
ADB3-5	0.0051	0.2032	0.0965	108	
ADB3-6	0.0330	0.6858	0.2286	2	35.33
ADB3-7	0.0127	0.1016	0.0762	108	28.87
ADB3-8	0.0152	0.6096	0.1092	30	34.95
ADB4-1	0.0432	0.4064	0.1270	4	35.76
ADB4-2	0.0254	0.3302	0.1270	5	35.33
ADB4-3	0.0064	0.3302	0.1270	9	38.35
ADB4-4	0.0165	0.3302	0.1397	40	35.77
ADB4-5	0.0127	0.3556	0.1270	10	17.08
ADB4-6	0.0178	0.4572	0.1524	11	14.89
ADB4-7	0.0254	0.3556	0.1270	14	16.18
ADB4-8	0.0406	0.5334	0.1016	12	16.89
ADB5-1	0.0356	0.3302	0.1270	0	12.99
ADB5-2	0.0406	0.3556	0.1651	2	13.42
ADB5-3	0.0254	0.4572	0.1524	3	13.28
ADB5-4	0.0229	0.4826	0.1397	9	1.23
ADB5-5	0.0356	0.1016	0.1270	60	15.19
ADB5-6	0.0229	0.5334	0.1270	0	27.36
ADB5-7	0.0254	0	0.1397	108	31.02
ADB5-8	0.0305	0.4826	0.1651	3	36.86
ADB6-1	0.0356	0.4318	0.1016	14	13.79
ADB6-2	0.0102	0.3302	0.1270	8	11.42
ADB6-3	0.0381	0.4826	0.1270	11	13.27
ADB6-4	0.0254	0.5334	0.1270	7	12.75
ADB7-1	0.0381				
ADB7-2	0.0254	0.5588	0.1524	20	15.51
ADB7-3	0.0381	0.635	0.1778	6	15.18
ADB7-4	0.3556	0.5842	0.1524	9	15.51
ADB8-1	0.0813	0.5334	0.1016	0	10.34
ADB8-2	0.0356	0.5842	0.1016	0	12.41
ADB8-3	0.0152	0.4318	0.1016	2	11.03
ADB8-4	0.0584	0.4572	0.1016	0	13.10
ADB9-1	0.0584	0.5588	0.1016	0	13.52
ADB9-2	0.0152	0.6096	0.1270	3	8.27
ADB9-3	0.0254	0.4826	0.1270	3	21.03
ADB9-4	0.0178	0.5588	0.1270	3	15.42

sample is a reliable indicator of the relation between the respective variables in the population. For example, a p level of 0.05 indicates that there a 5% probability that the relationship between the variables found in the samples is not related. In this study, a 1 minus p value was given along with the liner regression equation to indicate the related probability.

Correlation Coefficient R

The degree to which two or more variables are related to the dependent variables is expressed in the correlation coefficient R. In multiple regressions, R can assume values between 0 and 1. If there is no relationship between X and Y variables, then the ratio of the residual variability of the Y variable to the original variance is equal to 1.0. If X and Y are perfectly related then there is no residual variance and the ratio of variance would be 0. In most cases, the ratio should fall somewhere between these extremes, i.e., between 0 and 1. One minus this ratio is referred to as an R^2 of the coefficient of determination. This value can be interpreted in the following manner: if there is an R^2 of 0.4, then the variability of Y values around the regression line is 1–0.4 times the original variance; i.e., only 40% of the original variability can be explained.

Preliminary Examination Results

Diffusion brazing temperatures in the range of 899°C (1600°F) to 954°C (1700°F) for various lengths of time were used to conduct initial trials for establishing ADB process parameters. Three typical types of joint microstructures as shown in Fig. 5 (A, B, C) were observed. At lower brazing temperature and time, the ADB process resulted in a joint microstructure with three regions (I, II, and III as marked in Fig. 5A). In region I, an acicular/Widmanstätten structure was observed adjacent to the equiaxed $\alpha + \beta$ of the base metal. This was due to Cu and Ti (contained in the filler metal) diffusion into the base material, which lowered the β transus of the alloyed material in the joint and leads upon cooling to the formation of Widmanstätten structure throughout the joint. In region II, a full β structure was present again due to the β stabilization effect introduced by Cu and Ti. A trace of intermetallics was formed in region III as shown in Fig. 5A; the structure of this intermetallic phase was not identified at this stage. As an increase in temperature and time, region III diminished leaving the joint with full β structure as shown in Fig. 5B and $\alpha + \beta$ adjacent to the base metal. When the diffusion brazing temperature and time were further increased, a full $\alpha + \beta$ Widmanstätten microstructure in the joint (Fig. 5C) was formed and the $\alpha + \beta$ layer was moving further into the base metal due to the diffusion of elements from filler material, which will be discussed further.

A pressure between 689–1034 Pa (0.10–0.15 lb/in.^{2}) has proven to be adequate enough to ensure the brazing to occur while at same time not to deform the panel. One layer of foil did not seem to provide enough braze alloy to completely fill all the nodes and also caused considerable process variation. The effect of the number of filler metals was examined in more detail during the statistical study as described in the next sections. The effect of honeycomb core size was not investigated in the preliminary study.

Tensile Strength Test

Initially, the panels were bonded to the testing fixture using FM-1000 adhesive. However, the strength of the honeycomb panels exceeded the strength of the adhesive and fracture occurred within the adhesive joint. An Al brazing technique using Al 3003 foil was used to braze the ADB panels to the fixture. Three panels for each process condition were tested and the average tensile strength obtained was used in the linear regression. Ninety-five percent (R^2=0.95) of the test results were

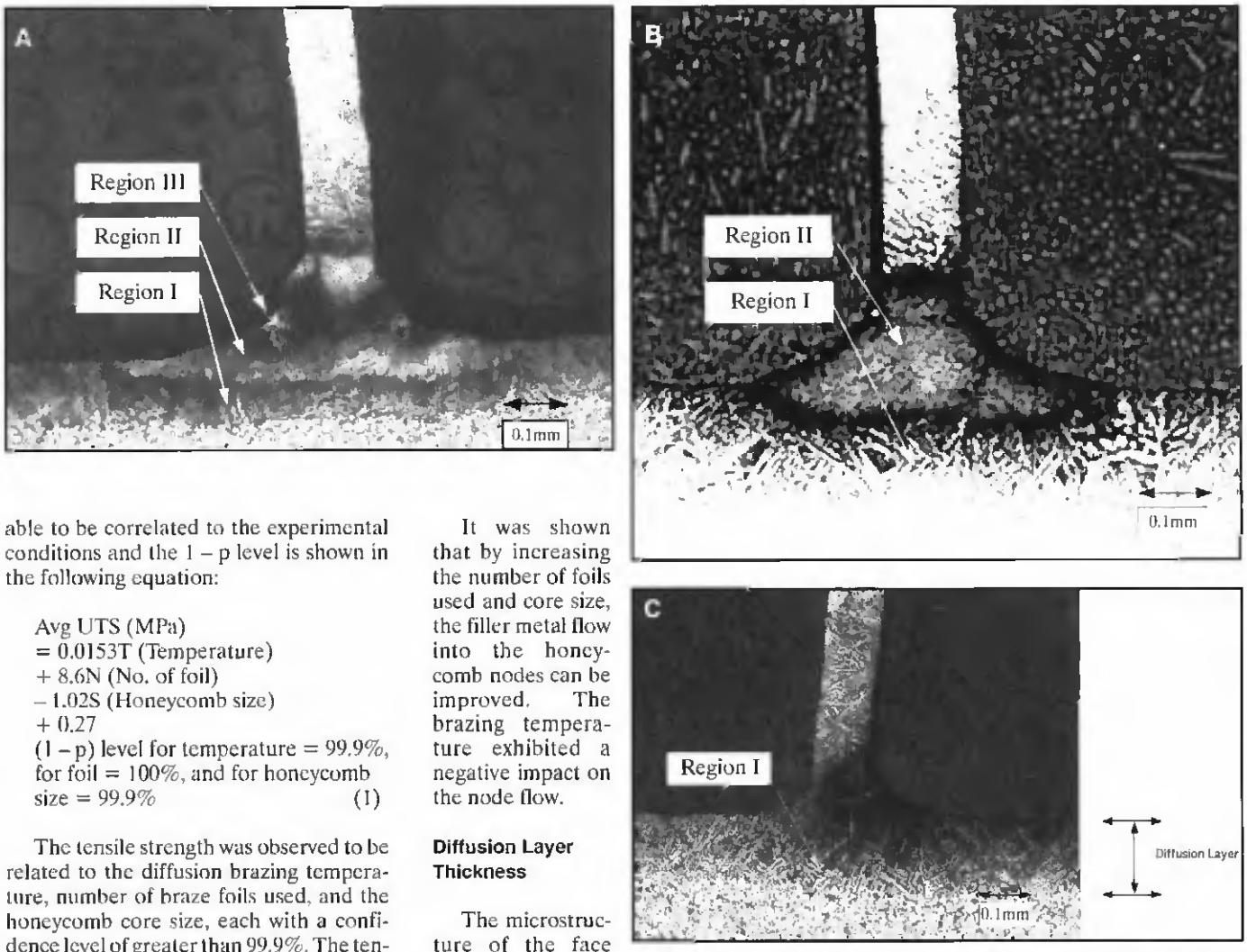

Fig. 5 — Microstructure of ADB joint. A — Incomplete diffusion with intermetallics; B — incomplete diffusion with single β phase region; C — α + β structure in the joint.

able to be correlated to the experimental conditions and the 1 – p level is shown in the following equation:

Avg UTS (MPa)
= 0.0153T (Temperature)
+ 8.6N (No. of foil)
– 1.02S (Honeycomb size)
+ 0.27
(1 – p) level for temperature = 99.9%, for foil = 100%, and for honeycomb size = 99.9% (1)

The tensile strength was observed to be related to the diffusion brazing temperature, number of braze foils used, and the honeycomb core size, each with a confidence level of greater than 99.9%. The tensile strength increases proportionally with temperature and number of foils used, and decreases with the honeycomb size.

The fracture surfaces were examined visually to find the failure locations. The majority of the panes failed within the honeycomb as shown in Fig. 6, with one panel (ADB 3–5) failing at the Al braze joint. The tensile strength in the later case was not considered in the analysis.

Filler Metal Flow

Filler metal flow to honeycomb nodes was evaluated using X-ray radiography and the number of nodes lacking filler metal on a 101 × 101 mm (4 × 4 in.) panel were counted. Only 43% of the population showed a strong relationship as expressed in Equation 2.

No. of Nodes lacking filler metal
= 0.097T (Temperature)
– 21.56N (No. of foil)
– 7.2S (Core size) + 1.728
(1 – p) level for temperature = 99.9%, for number of foil = 99.7%, and for core size = 99.9% (2)

It was shown that by increasing the number of foils used and core size, the filler metal flow into the honeycomb nodes can be improved. The brazing temperature exhibited a negative impact on the node flow.

Diffusion Layer Thickness

The microstructure of the face sheets (away from the fillet) showed two distinct layers. The first layer is the interdiffusion layer, where Cu and Ni atoms have diffused into the original equiaxed α plus intergranular β substrate and transformed the base microstructure into β structure which, on cooling, further transforms into α + β Widmanstätten structure. The next layer is the base material with equiaxed α + β structure as observed in the as-received material prior to joining. The thickness of the layers with α + β Widmanstätten microstructure is one of the measures to evaluate the extent of diffusion of filler metal into the base material (in this case the face sheet). The thickness of the diffusion layer (as illustrated in Fig. 5C) was measured on the polished and etched metallographic specimens and the measurements were normalized using face sheet thickness to prevent the variation resulting from specimen preparation (not perfectly normal to the cross section). The diffusion layer thickness was found to be strongly correlated ($R^2 = 0.95$) with heat treatment temperature, time, and also the amount of braze foil used. The 1 – p levels were well over 99% for all the independent variables as given below.

Diffusion Layer Thickness (mm) =
0.000046T (Temperature) +
0.00041t (Time) + 0.0185N
(No. of foil) + 0.0008
(1 – p) level for temperature = 99.9%, for time = 99.7%, and for number of foil = 99.6% (3)

An increase in temperature, time, and number of filler foils would result in thicker diffusion layer within the conditions employed in this study.

Fillet Size

The fillet size was evaluated by measuring both the fillet height and fillet width as defined in Fig. 2. It was found from statistical analysis that both of these depen-

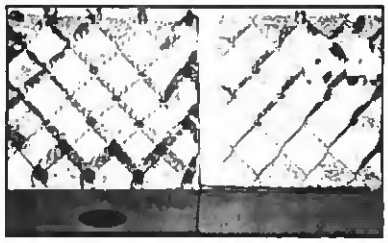

Fig. 6 — Fracture surface showing failure within the honeycomb core.

Table 2 — Effect of Brazing Temperature on the Joint Properties

	Temp.	Time	Face Sheet Thickness	Pressure	Filler Layer	Honeycomb Core Size
Tensile Strength	X				X	X
No. of H/C Nodes Lacking Flow	X				X	X
Diffusion Layer Thickness	X	X			X	
Fillet Size					X	X
Distortion	X		X			X

dent variables have similar correlation with the number of filler metal foils and honeycomb core size as shown in the following equation (with $R^2 = 0.095$):

Fillet height (mm) = 0.038N (Number of foil) + 0.0097S (Core size) (1 – p) level for number of foil = 99.9% and for core size = 99.9% (4)

Fillet Width (mm) = 0.21 N (Number of foil) + 0.045S (Core size) (1-p) level for number of foil and for core size = 100% (5)

As can be observed in Equations 4 and 5, the fillet size increased with the number of filler metal foils used and the honeycomb core size. The fillet size did not show any correlation with the brazing cycle parameters such as temperature, time, and pressure.

Distortion

The distortion of the face sheet after brazing showed certain correlation ($R^2 = 0.78$) with the temperature, face sheet thickness, and honeycomb core size as indicated in the following equation:

Distortion (mm) = 0.000046T (Temperature) – 0.0227f (Face sheet thickness) + 0.0015S (Core size) + 0.0008 (1-p) level for temperature = 99.9%, for face sheet thickness = 98.8%, and for core size = 86% (6)

Higher temperature and larger core size contributed to the increase in distortion, while the thicker face sheet improved the distortion. The reason for the relatively lower correlation coefficient will be discussed in the next section.

Discussion

The effects of all the variables (temperature, time, pressure, number of filler layers, face sheet thickness, and honeycomb size) on the various dependent variables (tensile strength, diffusion layer, fillet size, and distortion) previously detailed are summarized in Table 1. It can be observed from Table 2 that diffusion brazing temperature influenced all the dependent variables except fillet size. The cycle time only had an impact on the diffusion layer thickness, while face sheet thickness affected only the extent of distortion. Pressure within the range of 689–2068 Pa (0.1–0.3 lb/in.^{2}) did not seem to have any effect on the dependent variables investigated in this study, but the number of filler metal layers contributed significantly to the tensile strength, the number of nodes lacking braze alloy, diffusion layer thickness, and fillet size. Honeycomb size seems to impact most of the dependent variables. Utilization of the linear regression method has given a clear picture of the relationship between the processing parameters and the properties of diffusion brazed structures. However, the equations derived in this study are only applicable within the parameter ranges selected.

Tensile Strength

There has been very limited number of publications on diffusion brazing of Ti honeycomb structures. In one article, Ti honeycomb structure was brazed using amorphous CTEMET 1201 filler metal (11.5Zr-11.5Ni-23Cu-52Ti) (Ref. 17). The brazed honeycomb structure was tested and the tensile strength reported was near the base metal strength. No details on the relationship between the process parameters and the tensile strength of the brazed structure were reported.

In this study, factors found to have an impact on the tensile strength of the brazed panels were number of filler metal layers, temperature, and honeycomb core size. When the number of filler metal layers increased, the fillet size increased accordingly, and the number of nodes lacking filler metal was reduced as more filler metal was made available to fill the honeycomb nodes, as demonstrated in Equations 2, 4, and 5. Larger fillet size and reduced number of unfilled honeycomb nodes increased the effective loading cross section, resulting in increased tensile strength. The correlation between tensile strength and brazing temperature may be explained by the fact that the increase in temperature may promote a more homogeneous microstructure and eliminate the formation of intermetallics. Any adverse effect of grain growth on tensile strength with increase in temperature was not observed in this study. However, this needs to be examined further. The honeycomb core size, representing the cell wall spacing, is inversely proportional to the cell wall density. The increase in tensile strength in smaller honeycomb size is therefore due to its larger effective cross section compared to honeycomb with larger core size.

It is important to note that all the brazed panels failed in the honeycomb core, with the exception of one that failed between the panel and the fixture. By using ADB, the weakest link has been shifted from the joint (as commonly observed in the Al brazed structure) to the core. Further improvement to the structure strength can only be achieved with a better understanding of the process impact on core strength. It was reported (Ref. 18) that titanium honeycomb panels produced using diffusion brazing with an initial fine-grained core exhibited low structural strength as the brazing temperature was over the β-transus temperature and coarsening of the grain size occurred. Prebrazing annealing of the core material has shown improvement to the fatigue strength of diffusion brazed honeycomb panels. In another study, an increase in grain size of Ti sheet material from 6 μm to 9 μm was observed as a result of diffusion brazing at 940°C (Ref. 19). In this study, coarsening of grain size in comparison with the base material was observed in region 1 as shown in Fig. 5. However, as all the failures occurred in the honeycomb core, grain growth in the face sheet did not contribute to the tensile strength dependence on the processing parameters. Grain size coarsening in the core material was also observed and needs to be further investigated in a future study. The face sheet thickness was not observed to affect the tensile strength, which was consistent with the conclusion reported in another study (Ref. 19).

Honeycomb Node Flow

In manufacturing a honeycomb core, the individual walls are often joined using resistance spot welding to form nodes. During subsequent brazing or diffusion processes, filler metal is drawn into the honeycomb node once liquid is formed. The flow of filler metal into the honeycomb nodes further joins the honeycomb walls and at the same time forms a braze between the honeycomb core and the face sheets. One of the reasons that solid-state diffusion brazing is not applicable in manufacturing of honeycomb structures is that there is no means to fill the nodes. The flow of filler metal into the nodes is routinely used in the aerospace industry as an evaluation standard for honeycomb structures. In this study, it has been shown in Equation 2 that the number of nodes lacking filler metal is reduced with additional filler metal and a reduction in the total number of nodes present (as in the case of larger core size). The confidence level was, however, lower as compared to the other measurements. This may be attributed to the variation in honeycomb core thickness, which was not taken into consideration. As intimate contact between the filler metal and core surface is essential in ADB processing to achieve a braze and obtain filler metal flow into the honeycomb nodes, any variation in core thickness could lead to lack of filler metal flow into the nodes and a poor joint between face sheet and core. Trials were initiated to machine/level the core surface prior to diffusion brazing, but this is beyond the scope of this study.

Diffusion Layer Thickness

According to Fick's second law, the concentration of the diffusing element at a given position x is expressed as

$$c(x,t) = \frac{M}{2\sqrt{\pi Dt}} \exp\left(-\frac{x2}{4Dt}\right) \quad (7)$$

The diffusion coefficient is calculated using

$$D = D_0 \exp\left(-\frac{Q}{RT}\right) \quad (8)$$

The diffusion distance at $c = 0$ can be estimated as

$$x = 2\sqrt{Dt} \quad (9)$$

where M is the total amount of interlayer, D is the interdiffusion coefficient, T is the temperature, t is the time, and Q is the diffusion activation energy.

The diffusion of filler metal into the base metal increases with the brazing temperature and time as shown in Equations 8 and 9. The diffusion thickness measured in this study showed the same trend as given in Equation 3, however in a linear manner. The regression equation also indicated that the diffusion layer is proportional to the amount of filler metal used, which can be explained by the fact that M in Equation 7 is greater. The face sheet thickness and honeycomb core size did not show any influence on the diffusion layer thickness as they do not contribute to the extent of diffusion and concentration gradient.

In order to look at the diffusion of filler metal into the base metal in a quantitative way, for example Ni diffusion into Ti, Equation 9 can be used to estimate the diffusion distance. Assuming $D = 3 \times 10^{-12}$ m^2s^{-1} (Ni diffuse into β Ti at 900°C) (Refs. 20, 21), the estimated diffusion distance is about 0.21 mm (0.0084 in.) after diffusion brazing at 900°C for 60 min. The average diffusion layer thickness (defined as the thickness of layer with α + β Widmanstätten structure) for panels joined at 899°C (1650°F) was 0.08 mm (0.0034 in.), which is not in an agreement with the calculated value. It can be explained as 1) Ni diffused further into the base metal without causing observed microstructure changes; 2) the Ni concentration was not maintained at a constant value once the diffusion started because a thin foil was used. The first explanation was confirmed in a recent study (to be published) using SEM/EDS where it was found that as high as 2.6% Ni can be present in the base metal without causing microstructure changes. A detailed study of the diffusion of the filler metal is being conducted.

Additional factors such as heating rate on diffusion layer were observed during diffusion brazing of Ti-6Al-4V to stainless steel using copper foil. It was observed that the width of α + β eutectoid transformation zone increased as a result of a decrease in heating rate and increase in holding time (Ref. 22). As constant heating and cooling rates were used in this study, their effects were not evaluated.

Fillet Size

Fillet size is determined primarily by the amount of filler metal available and the density of honeycomb walls (honeycomb single walls and nodes) to be brazed onto the face sheet as shown in Equations 4 and 5. The smaller the honeycomb core size, the lesser the fillet size as there were more walls and nodes to be joined. The observed fillet size also showed a strong dependence on the number of filler metal foils used. With an increase in filler metal layer, there will be more material made available to form a larger fillet. There is a trade-off, however, that needs to be considered here. Although a larger fillet may reinforce the joint, this would cause an increase in diffusion layer thickness and formation of intermetallic when diffusion brazing at the same temperature and time. The design of the ADB process must be such that filler metal is controlled to the minimum necessary to achieve the required fillet size. It is also worth noting that Equations 4 and 5 indicate that the temperature and time used did not affect the fillet size.

Distortion

Distortion of the face sheet that occurred during the ADB cycle could have been caused by the following factors: 1) pressure applied to the panel, 2) face sheet thickness, 3) cooling rate from brazing cycle, 4) honeycomb size, and 5) brazing temperature. The linear regression Equation 6 demonstrated that the distortion was associated with temperature, face sheet thickness, and honeycomb core size and not related to pressure applied and cooling rate. In the initial study, it was observed that the cooling rate, if not designed adequately, could cause heavy buckling of the face sheet. In this study, the cooling rate was set to a constant value and therefore did not contribute to the difference in distortion. The pressure applied to the panel in the range of 689–2068 Pa (0.1–0.3 lb/in.^{2}) did not seem to have any effect on the distortion. The low correlation coefficient associated with distortion and process parameters could again be related to the core thickness variations. It is suggested that the core material must be carefully examined and prepared prior to the diffusion brazing process in order to fully investigate the process effect.

Conclusions

An ADB process was investigated and successfully used for manufacture of Ti honeycomb structures. A method to estimate key properties required for process control of honeycomb structures based on the process parameters was developed using DOE and linear regression. The linear regression equations derived can also be used to provide process parameters when design requirements, such as core size, face sheet thickness, minimum strength, and maximum distortion, are given. Thus, from the above analysis key process characteristics influencing each mechanical property can be evaluated in a statistically significant manner, leading to the ability to establish a robust manufacturing ADB process. This should lead to more confidence in the process and encourage engineers to consider ADB as a viable process for the manufacture of Ti honeycomb structures. The approach used in this study would also be applicable

to other metal-honeycomb structures such as for using Ni alloys with temperatures in excess of the capability of Ti alloys.

Additionally, the following conclusions can be made with respect to each property evaluated:

1) The tensile strength of the brazed panels increased with the brazing temperature, number of filler metal layers, and honeycomb core density.

2) The number of nodes lacking filler metal showed some relationship with temperature, number of filler metal layers, and honeycomb core.

3) The diffusion layer thickness increased with temperature, time, and number of filler metal layers, which is consistent with the diffusion mechanism.

4) Fillet size was observed to be affected only by number of filler metal layers and honeycomb core size.

5) The face sheet distortion of the honeycomb structure increased with temperature and honeycomb core size and decreased with face sheet thickness.

6) The pressure applied to the honeycomb core did not affect any of the variables examined in this study.

Further Study

As detailed in the results and discussion section, only a preliminary analysis of the microstructure was conducted. Further analysis is being undertaken to study the microstructure evolution in the joint and base metal (core and face sheet), including diffusion of filler metal into the base metal. Upon achieving a full understanding of the microstructure, further trials will be initiated to modify the chemical composition of the filler metal and process parameters to explore the possibility of producing microstructure similar to the base metal in the brazed joint.

Reference

1. Paik, J. K., Thayambilli, A. K., and Kim, G. S. 1999. The strength characteristics of aluminum honeycomb sandwich panels. *Thin-Walled Structures* 35: 205–231.

2. Suslov, A. A. 1995. Brazing laminated structures of light alloys based on aluminum and titanium. *Welding International* 9(7): 570–572.

3. Well, R. R. 1975. Low temperature large-area brazing of damage tolerant titanium structures. *Welding Journal* 54(10): 348–356.

4. Berger, D. D. 1995. Vacuum brazing titanium to Inconel. *Welding Journal* 74(11): 35–38.

5. Lynch, J. F., Feinstein, L., and Huggins, R. A. 1959. *Welding Journal* 38(2): 85-s to 89-s

6. Wu, K. C. 1971. *Welding Journal* 50(9): 386-s to 393-s.

7. Chang, E., and Chen, C.-H. 1997. Low-melting-point titanium-base brazing alloys — Part 2: Characteristics of brazing Ti-21Ni-14Cu on Ti-6Al-4V substrate. *Journal of Materials Engineering and Performance* 6(6): 797–803.

8. Rabinkin, A., Liebermann, M., Pounds, A., Taylor, T., Reidinger, F., and Lui, S.-C. 1991. Amorphous Ti-Zr-base Metglas brazing filler metals. *Scr. Metal.* 25 (2): 399–404.

9. Botstein, O., and Rabinkin, A. 1994. Brazing of titanium-based alloys with amorphous 25%Ti-25%Zr-50%Cu filler metal. *Materials Science and Engineering* A. 188: 305–315.

10. Fukumoto, S., Kasahara, A., Hirose, A., and Kobayashi K. F. 1994. Transient liquid phase bonding of continuous SiC fiber reinforced Ti-6Al-4V composite to Ti-6Al-4V alloy. *Materials Science and Technology* 10(9): 807–812.

11. Moris, B. 1986. *Conf. Proc. on Designing with Titanium*, pp. 83-86, Inst. of Metals.

12. Fitzpatrick G. A., and Broughton, T. 1986. *International Conference on Titanium Product and Applications*. San Francisco, Calif.

13. Fitzpatick, G. A. 1992. Application of diffusion bonding in the manufacturing of aeroengine components. *Int. SAMPE Metals and Metal Processing Conf.* 3: 622–628.

14. Lan, S.W. 1982. Laminated brazing filler metals for titanium assemblies. *Welding Journal* 61(10): 23–28.

15. Chang E., and Chen, C.-H. 1997. Low-melting-point titanium-base brazing alloys — Part I: Characteristics of two-, three- and four-component filler metals. *Journal of Materials Engineering and Performance* 6(6): 792–796.

16. Wilbey, A., and Ward-Close, C. M. 1994. Diffusion bonding of the high temperature Ti alloy IMI 829 to Fe-Ni alloys IN907 using interlayers. *Materials Letters* 21(1): 47–53.

17. Kalin, B. A., Sevryukow, O. N., Fedotov, V. T., and Triggered, A. E. 1997. Brazing thin sheet structure of titanium alloys using CTEMET amorphous brazing alloys. *Welding International* 11(6): 234–235.

18. Kolomenskii, A. B., Salikov, V. A., Roshchupkin, A. N., and Degtyarev, A. V. 1995. Efficiency of titanium honeycomb packets produced by diffusion bonding. *Welding International* 9(9): 742–744.

19. Islam, M. F., Piling, J., and Ridley, N. 1997. Effect of surface finish and sheet thickness on isostatic diffusion bonding of superplastic Ti-6Al-4V. *Materials Science and Technology* 13(12): 1045–1050.

20. Hinotani, B., and Ohmori, Y. 1988. The microstructure of diffusion-bonded Ti/Ni interface. *Transaction of the Japan Institute of Metals* 29(2): 116–124.

21. Aleman, A., Gutierres, I., and Urcola, J. J. 1995. Interface microstructures in the diffusion bonding of a titanium alloy to Inconel 625. *Met. Trans.* 26A (2): 437–446.

22. Eroglu, M., Khan, T. I., and Orhan, N. 2002. Diffusion bonding between Ti-6Al-4V and microduplex stainless steel with copper interlayer. *Materials Science and Technology* 18(1): 68–71.

Appendix 1

Design of Experiment

For a given honeycomb cell size and thickness, the effect of changing filler metal layers (N), face sheet thickness (f), temperature (T), time (t), and pressure (P) was assessed. If only one temperature/time combination is tested, then any difference found may be due to a day effect rather than a true temperature/time effect. Therefore, to test a day effect, a reduced number of experiments on cell size S = 6.4 mm (¼ in.) was run on different days as follows:

Set 1 (Temperature at T½ and f = f_0 and N = N_0)

t_0P_0 t_0P_1 t_0P_0 t_0P_1
t_1P_0 t_1P_1 t_1P_0 t_1P_1

Set 2

t_0P_0 t_0P_1 t_0P_0 t_0P_1
t_1P_0 t_1P_1 t_1P_0 t_1P_1

Where 0 = lower level, ½ = middle level and 1 = high level and defined as:

Filler metal layers
N_0=1 layer, N½ = 2 layers, N_1 = 3 layers

Face sheet thickness
f_0 = 0.38 mm (0.015 in.), f½ = 0.64 mm (0.025 in.), f_1 = 1.19 mm (0.047 in.)

Brazing temperature
T_0 = 899°C (1650°F), T½ = 926°C (1700°F)
T_1 = 954°C (1750°F).

Brazing cycle time
0 = 60 min., t½ = 90 min., t_1 = 120 min.

Pressure
P_0 = 689 Pa (0.1 lb/in.^{2}), P½ = 1379 Pa (0.2 lb/in.^{2}), P_1 = 2068 Pa (0.3 lb/in.^{2})

For cell size S = 3.18 mm (⅛ in.), an experiment of 12 runs designed with replicated points was used as

Set 3 (T = T½, f = f_0)

$N_0t_0P_0$ $N_1t_0P_0$ $N_0t_0P_1$ $N_0t_1P_0$
$N_1t_0P_1$ $N_1t_1P_0$ $N_0t_1P_1$ $N_1t_1P_1$
N½t½P_0 N½t½P_0 N½t½P_1 N½t½P_1

For cell size S = 9.53 mm (⅜ in.), a full factorial design with replicated center points required 20 runs as follows:

Set 4 (N = N_0)

$f_0T_0t_0P_0$ $f_1T_0t_0P_0$ $f_0T_1t_0P_0$ $f_0T_0t_1P_0$
$f_0T_0t_0P_1$ $f_1T_1t_0P_0$ $f_1T_0t_1P_0$ $f_1T_0t_0P_1$
$f_0T_1t_1P_0$ $f_0T_1t_0P_1$ $f_0T_0t_1P_1$ $f_1T_1t_1P_0$
$f_1T_1t_0P_1$ $f_1T_0t_1P_1$ $f_0T_1t_1P_1$ $f_1T_1t_1P_1$
f½T½t½P½ F½T½t½P½
f½T½t½P½

Appendix 2

Tables (2-1 to 2-9) — Parameters Used for Diffusion Brazing Trials

2-1

	Temp (°C)	Time (min.)	Face Sheet Thickness (mm)	Pressure (Pa)	No. of Foils	Core Size (mm)
ADB1-1	899	60	0.38	689	1	9.53 core
ADB1-2	899	60	1.19	689	1	9.53 core
ADB1-3	899	60	0.38	2068	1	9.53 core
ADB1-4	899	60	1.19	2068	1	9.53 core

2-2

	Temp (°C)	Time (min.)	Face Sheet Thickness (mm)	Pressure (Pa)	No. of Foils	Core Size (mm)
ADB2-1	899	60	1.19	689	1	9.53 core
ADB2-2	899	60	0.38	2068	1	9.53 core
ADB2-3	899	60	1.19	2068	1	9.53 core
ADB2-4	899	60	0.38	689	1	9.53 core

2-3

	Temp (°C)	Time (min.)	Face Sheet Thickness (mm)	Pressure (Pa)	No. of Foils	Core Size (mm)
ADB3-1	926	60	0.38	689	1	6.35 core
ADB3-2	926	60	0.38	2068	1	6.35 core
ADB3-3	926	60	0.38	689	1	6.35 core
ADB3-4	926	60	0.38	2068	1	6.35 core
ADB3-5	926	60	0.38	689	1	3.18 core
ADB3-6	926	60	0.38	689	3	3.18 core
ADB3-7	926	60	0.38	2068	1	3.18 core
ADB3-8	926	60	0.38	2068	3	3.18 core

2-4

	Temp (°C)	Time (min.)	Face Sheet Thickness (mm)	Pressure (Pa)	No. of Foils	Core Size (mm)
ADB4-1	926	90	0.38	689	2	3.18 core
ADB4-2	926	90	0.38	689	2	3.18 core
ADB4-3	926	90	0.38	2068	2	3.18 core
ADB4-4	926	90	0.38	2068	2	3.18 core
ADB4-5	926	90	0.64	1379	1	9.53 core
ADB4-6	926	90	0.64	1379	1	9.53 core
ADB4-7	926	90	0.64	1379	1	9.53 core
ADB4-8	926	90	0.64	1379	1	9.53 core

2-5

	Temp (°C)	Time (min.)	Face Sheet Thickness (mm)	Pressure (Pa)	No. of Foils	Core Size (mm)
ADB5-1	926	120	0.38	689	1	6.35 core
ADB5-2	926	120	0.38	2068	1	6.35 core
ADB5-3	926	120	0.38	689	1	6.35 core
ADB5-4	926	120	0.38	2068	1	6.35 core
ADB5-5	926	120	0.38	689	1	3.18 core
ADB5-6	926	120	0.38	689	3	3.18 core
ADB5-7	926	120	0.38	2068	1	3.18 core
ADB5-8	926	120	0.38	2068	3	3.18 core

2-6

	Temp (°C)	Time (min.)	Face Sheet Thickness (mm)	Pressure (Pa)	No. of Foils	Core Size (mm)
ADB6-1	954	60	0.38	689	1	9.53 core
ADB6-2	954	60	1.19	2068	1	9.53 core
ADB6-3	954	60	1.19	689	1	9.53 core
ADB6-4	954	60	0.38	2068	1	9.53 core

2-7

	Temp (°C)	Time (min.)	Face Sheet Thickness (mm)	Pressure (Pa)	No. of Foils	Core Size (mm)
ADB7-1	954	120	0.38	689	1	9.53 core
ADB7-2	954	120	1.19	689	1	9.53 core
ADB7-3	954	120	0.38	2068	1	9.53 core
ADB7-4	954	120	1.19	2068	1	9.54 core

2-8

	Temp (°C)	Time (min.)	Face Sheet Thickness (mm)	Pressure (Pa)	No. of Foils	Core Size (mm)
ADB8-1	926	60	0.38	689	1	6.35 core
ADB8-2	926	60	0.38	2068	1	6.35 core
ADB8-3	926	60	0.38	689	1	6.35 core
ADB8-4	926	60	0.38	2068	1	6.35 core

2-9

	Temp (°C)	Time (min.)	Face Sheet Thickness (mm)	Pressure (Pa)	No. of Foils	Core Size (mm)
ADB9-1	926	120	0.38	689	1	6.35 core
ADB9-2	926	120	0.38	2068	1	6.35 core
ADB9-3	926	120	0.38	689	1	6.35 core
ADB9-4	926	120	0.38	2068	1	6.35 core